UC Santa Barbara
UC Santa Barbara Previously Published Works

Title
Excitation wavelength dependence of terahertz emission from InN and InAs

Permalink
https://escholarship.org/uc/item/5jz3h5xg

Journal
Applied Physics Letters, 89(14)

ISSN
0003-6951

Authors
Chern, G D
Readinger, E D
Shen, H G
et al.

Publication Date
2006-10-01

Peer reviewed

eScholarship.org Powered by the California Digital Library
University of California

Excitation wavelength dependence of terahertz emission from InN and InAs

Grace D. Chern,[a] Eric D. Readinger, Hongen Shen, and Michael Wraback
U.S. Army Research Laboratory, Sensors and Electron Devices Directorate, AMSRD-ARL-SE-EM, 2800 Powder Mill Road, Adelphi, Maryland 20783

Chad S. Gallinat, Gregor Koblmüller, and James S. Speck
Materials Department, University of California, Santa Barbara, California 93106-5050

(Received 9 May 2006; accepted 17 August 2006; published online 3 October 2006)

The authors report on the excitation wavelength dependence of terahertz emission from *n*-InN and bulk *p*-InAs pumped with femtosecond pulses tunable from 800 to 1500 nm. The terahertz amplitude, normalized to pump and probe power, from both narrow band gap semiconductors remains relatively constant over the excitation wavelength range. In addition, terahertz radiation from In- and N-face InN samples with bulk carrier concentrations ranging from 10^{17} to 10^{19} cm^{-3} is also investigated, showing a strong dependence of terahertz emission on bulk carrier concentration. The experimental results agree well with calculations based on drift-diffusion equations incorporating momentum conservation and relaxation. © *2006 American Institute of Physics*. [DOI: 10.1063/1.2358938]

The terahertz region of the electromagnetic spectrum, lying between microwave frequencies (100 GHz) and photonic frequencies (30 THz), is a potentially important region for a wide variety of applications, including imaging, time-domain spectroscopy, and material identification and characterization.[1–3] Traditionally, optically generated terahertz systems utilize femtosecond mode-locked Ti: sapphire lasers or continuous-wave (cw) lasers with a wavelength centered near 800 nm. Significant advantages associated with the use of telecommunications grade optoelectronics and compact fiber lasers could be gained in cost, size, weight, and efficiency by shifting the wavelength to 1550 nm if an appropriate narrow band gap semiconductor terahertz source were available. In addition, for cw terahertz generation obtained by photomixing (or optical heterodyne conversion), 1550 nm operation is advantageous because the photomixing conversion efficiency, which increases as λ^2, is about four times higher than for conventional terahertz systems using 800 nm. Terahertz generation using compact fiber laser systems has already been demonstrated with InAs, InSb, and GaAs.[4–6]

High quality InN thin films exhibit a band gap E_g below[7] 0.7 eV, a much smaller value than what was previously accepted (E_g=1.9 eV or λ=650 nm).[8] Recently, we have measured using absorption data an InN band gap below 0.65 eV in compressively strained InN films on GaN templates.[9] Estimates of the deformation potential point to an unstrained band gap of ~0.63 eV. By constructing InN/GaInN quantum well structures, it should be possible to engineer a material with a band gap close to 1550 nm for use with low-cost, 1550 nm lasers. Unlike conventional III-V semiconductor compounds, wurtzite III-nitride semiconductors possess a significant spontaneous polarization, leading to an internal electric field in quantum wells about an order of magnitude larger than that found in conventional III-V materials.[10] This phenomenon combined with a high saturation velocity ($>1.5\times10^7$ cm/s),[11] large intervalley spacing to confine carriers within the high mobility Γ valley, short carrier lifetime, and potentially high breakdown voltage in InN may lead to up to an order of magnitude higher efficiency InN-based terahertz sources compared with the commonly employed arsenides.

Recently, Adomavicius *et al.*[12] have measured the spectral dependence of terahertz emission from (111) InAs at high carrier densities, where nonlinear effects are the dominant terahertz generation mechanism. Such high optical fluences, however, are not suitable for compact fiber lasers. Additionally, at lower carrier densities, the optical rectification contribution is no longer the main terahertz generation mechanism in (111) InAs, but becomes comparable to effects due to the difference of the electron and hole diffusion coefficients (photo-Dember effect).[13]

The possibility of terahertz emission from InN has been demonstrated by Ascazubi *et al.*,[14] who attributed the terahertz generation mechanism to transient photocurrents but did not specify the exact mechanism. Similar to InAs, InN has a surface accumulation layer, which has a width that is more than an order of magnitude shorter than the optical absorption length.[15] The high surface state density leads to a high field near the surface but virtually no field in the bulk of the crystal. The optically induced transient photocurrents in InN should therefore be similar to InAs, that is, due to the photo-Dember effect.

In this letter, we present a comparison of terahertz emission from *n*-InN and bulk *p*-InAs, one of the best known terahertz semiconductor surface emitters, excited with ultrafast laser pulses at wavelengths tuned between 800 and 1500 nm. The terahertz radiation generated from InAs and InN exhibits similar dependence on the excitation wavelength. The terahertz amplitude from both narrow band gap semiconductors remains on the same order of magnitude, while the pump wavelength is tuned from 800 to 1500 nm. At a fixed pump wavelength, the terahertz amplitude from *n*-InN is about an order of magnitude smaller than for *p*-InAs due to larger screening from *n* type as compared to *p*-type carriers, as well as larger screening due to a larger density of background electrons in the *n*-InN than background holes in the *p*-InAs. Terahertz radiation from In-

[a]Electronic mail: grace.chern@arl.army.mil

 © 2006 American Institute of Physics
Downloaded 25 Apr 2007 to 128.111.179.5. Redistribution subject to AIP license or copyright, see http://apl.aip.org/apl/copyright.jsp

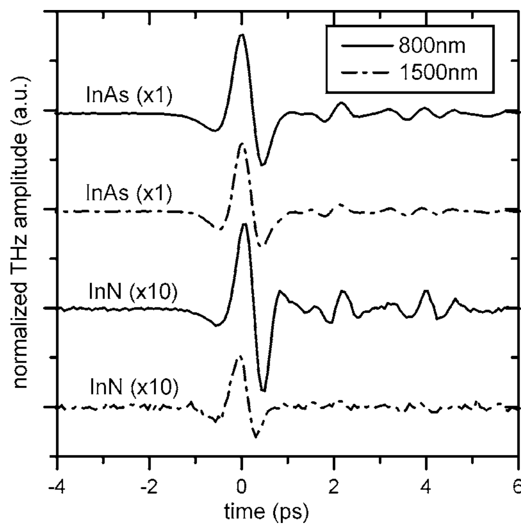

FIG. 1. Time-domain wave forms of terahertz emission, normalized to pump and probe power, from bulk p-type InAs and In-face n-InN excited with 800 nm (solid line) and 1500 nm (dashed line) femtosecond pulses.

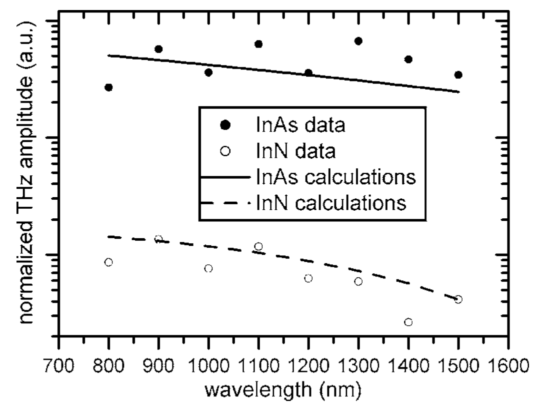

FIG. 2. Excitation wavelength dependence of terahertz amplitude, normalized to pump and probe power, from InN and InAs. The points indicate experimental data (solid circles: InAs and empty circles: InN) and lines indicate calculated results (solid: InAs and dashed: InN).

(Ref. 9) and N-face[16] n-InN samples with a bulk carrier concentration n_{bulk} ranging from 10^{17} to 10^{19} cm^{-3} is examined and shows a significant decrease as n_{bulk} increases. These results are consistent with the dominant mechanism for terahertz generation in InN and InAs being the current associated with the diffusion of the photogenerated electrons at elevated electron temperature (photo-Dember effect) and the redistribution of the background electrons under drift.

Our measurements are performed using a Coherent regenerative amplifier (RegA) system, which operates at 800 nm and has a repetition rate of 250 kHz. The output of the RegA is split into two beams. The stronger beam is frequency doubled to serve as the pump source for an optical parametric amplifier, which generates an infrared idler pulse tunable from 0.9 to 2.6 μm. The infrared beam, after compression with a prism pair to typical pulse widths of $\sim$150 fs, is then focused onto the semiconductor sample at a 45° incidence angle with a beam diameter of $\sim$1 mm. The pump power is $\sim$4 mW for all excitation wavelengths. The subsequent terahertz emission from the semiconductor surface is collected with a pair of parabolic mirrors onto a ZnTe crystal for electro-optic sampling. The weaker RegA split-off beam is used to probe the terahertz emission for all excitation wavelengths, as well as to irradiate the samples at 800 nm.

The n-InN sample used for the excitation wavelength dependence measurements is a 1-μm-thick In-face film grown by molecular beam epitaxy on an Fe-doped GaN template with a GaN buffer layer. Details of the growth technique are described elsewhere.[9] The unintentionally doped n-InN sample has a bulk carrier concentration of 2.25×10^{17} e/cm^3, a Hall mobility of 2098 cm^2/V s, and a threading dislocation density of $\sim 3 \times 10^{10}$ cm^{-2} (as determined by x-ray diffraction and transmission electron microscopy measurements). A description of the growth technique for the N-face InN samples can be found in Ref. 16. The p-type (111) InAs sample is 450 μm thick with a doping level of $\sim 10^{16}$ cm^{-3}.

Figure 1 shows the time-domain wave forms of the terahertz emission, normalized to pump and probe power, from bulk p-type InAs and n-InN optically excited with 800 nm (solid line) and 1500 nm (dashed line) femtosecond pulses. For both semiconductors, the terahertz amplitude at 800 nm is comparable to the signal amplitude at 1500 nm. This result is reflected in the systematic measurements of the terahertz emission from InAs and InN at excitation wavelengths varying from 800 to 1500 nm displayed in Fig. 2. Measurements of terahertz emission as a function of azimuthal angle (about the surface normal) indicate that the optical rectification component is small ($<10\%$) for InAs and negligible for InN.

A one-dimensional momentum conservation and relaxation equation,

$$\frac{\partial J_n}{\partial t} = e\left(n\frac{eE}{m^*} + \frac{kT}{m^*}\frac{\partial n}{\partial x}\right) - \frac{J_n}{\tau}, \tag{1}$$

with a k-dependent effective mass[17] m^* is used to simulate the subpicosecond electron current density J_n. The parameters e, n, E, T, and τ are the elementary electric charge, carrier concentration, electric field, carrier temperature, and momentum relaxation time, respectively. Photogenerated and background electron currents are calculated separately due to their different carrier temperatures. Both the photogenerated and background hole currents are calculated using drift-diffusion equations assuming that their temperatures are invariant at room temperature. These equations with carrier conservation equations are solved using a modified Scharfetter-Gummel scheme.[18] The emitted terahertz signal is then calculated as the volume integration of the time derivative of the total current density.

Modeling shows that the dominant currents are the diffusion of the photogenerated electrons at elevated electron temperature [the second term on the right hand side of Eq. (1)] and the redistribution of the background electrons under drift effect [the first term on the right hand side of Eq. (1)]. As the excitation wavelength increases, the photoexcited electron temperature decreases, thereby lowering the terahertz amplitude. However, the photon number increases as the excitation wavelength increases, enhancing the terahertz amplitude. As the excitation wavelength goes from 800 to 1500 nm for InN, the photoexcited electron temperature decreases by a factor of 5 while the photon number increases by a factor of $\sim$1.9, producing an overall decrease of less than four times. The decrease in terahertz signal for InN is only slightly larger than for p-InAs (E_g=0.36 eV),

Downloaded 25 Apr 2007 to 128.111.179.5. Redistribution subject to AIP license or copyright, see http://apl.aip.org/apl/copyright.jsp

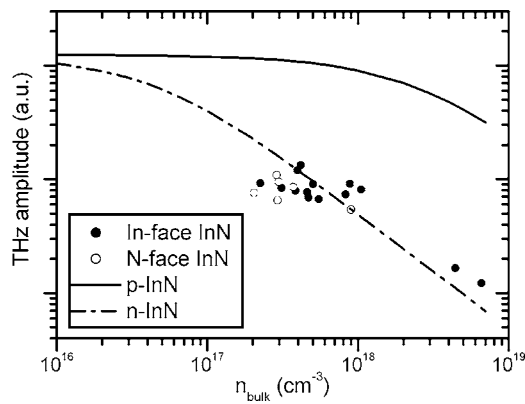

FIG. 3. Terahertz amplitude dependence on bulk carrier density n_{bulk} for In- (solid circles) and N-face (empty circles) InN samples optically excited with 800 nm femtosecond pulses. Calculated results for p-type and n-type InN are shown with solid and dashed lines, respectively.

where the photoexcited electron temperature decreases by a factor of 2.5, giving an overall decrease in signal amplitude of less than two times from 800 to 1500 nm. The experimental results agree well with calculations (solid and dashed lines in Fig. 2).

The measured terahertz amplitude from n-InN is about an order of magnitude smaller than from p-InAs due to larger screening from the higher mobility electrons as compared to holes. For example, at the fixed bulk carrier concentration of 10^{18} cm^{-3}, the calculations in Fig. 3 show that the terahertz amplitude from p-InN would be more than an order of magnitude larger than from n-InN. The higher density of background carriers in the InN sample, as compared to InAs, also contributes to the larger screening effect. As seen in Fig. 3, the measured normalized terahertz amplitude from InN decreases by about one order of magnitude as the bulk carrier concentration n_{bulk} increases by one order of magnitude. Although there are several other effects which contribute to the terahertz amplitude, including photoexcited electron temperature, mobility, absorption, and carrier lifetime, screening from carriers appears to be the dominant effect. There is no discernable difference between the In- and N-face InN samples, as expected for the improved crystalline quality and concomitant low background electron density and high mobility for both polarities.[9,16] Liu *et al.*[13] have shown a similar dependence on carrier concentration for the terahertz radiation from InAs.

In summary, we have demonstrated a similar excitation wavelength dependence of terahertz emission from n-InN and bulk p-InAs excited with femtosecond laser pulses. When the excitation wavelength is tuned from 800 to 1500 nm, the terahertz amplitude from both narrow band gap semiconductors remains on the same order of magnitude. The terahertz amplitude from n-InN is about an order of magnitude smaller than for p-InAs due to larger screening from n-type as compared to p-type carriers, as well as a higher density of background electrons in InN than background holes in p-InAs. It is expected that the terahertz power from InN will improve with lower n-type bulk carrier concentration or p-type doping, as well as with manipulation of the large built-in electric fields associated with the spontaneous and piezoelectric polarizations in this material.

This research was supported in part by an appointment to the U.S. Army Research Laboratory Postdoctoral Fellowship Program administered by the Oak Ridge Associated Universities through a contract with the U.S. Army Research Laboratory. The work at the University of California, Santa Barbara was supported by DARPA (CNID program) and AFOSR (D. J. Silversmith, program manager).

[1] D. Grischkowsky, S. Keiding, M. van Exter, and C. Fattinger, J. Opt. Soc. Am. B **7**, 2006 (1990).
[2] B. B. Hu and M. C. Nuss, Opt. Lett. **20**, 1716 (1995).
[3] D. M. Mittleman, R. H. Jacobsen, and M. C. Nuss, IEEE J. Sel. Top. Quantum Electron. **2**, 679 (1996).
[4] H. Ohtake, Y. Suzuki, N. Sarukura, S. Ono, T. Tsukamoto, A. Nakanishi, S. Nishizawa, M. L. Stock, M. Yoshida, and H. Endert, Jpn. J. Appl. Phys., Part 2 **40**, L1223 (2001).
[5] H. Takahashi, Y. Suzuki, M. Sakai, S. Ono, N. Sarukura, T. Sugiura, T. Hirosumi, and M. Yoshida, Appl. Phys. Lett. **82**, 2005 (2003).
[6] M. Nagai, K. Tanaka, H. Ohtake, T. Bessho, and T. Sugiura, Appl. Phys. Lett. **85**, 3974 (2004).
[7] J. Wu, W. Walukiewicz, K. M. Yu, J. W. Ager III, E. E. Haller, H. Lu, W. J. Schaff, Y. Saito, and Y. Nanishi, Appl. Phys. Lett. **80**, 3967 (2002).
[8] T. Tansley and C. P. Foley, J. Appl. Phys. **59**, 3241 (1986).
[9] C. S. Gallinat, G. Koblmüller, J. S. Brown, S. Bernardis, J. S. Speck, G. D. Chern, E. D. Readinger, H. Shen, and M. Wraback, Appl. Phys. Lett. **89**, 032109 (2006).
[10] F. Bernardini, V. Fiorentini, and D. Vanderbilt, Phys. Rev. B **56**, R10024 (1997).
[11] S. K. O'Leary, B. E. Foutz, M. S. Shur, and L. F. Eastman, Appl. Phys. Lett. **87**, 222103 (2005).
[12] R. Adomavicius, G. Molis, A. Krotkus, and V. Sirukaitis, Appl. Phys. Lett. **87**, 261101 (2005).
[13] K. Liu, J. Xu, T. Yuan, and X.-C. Zhang, Phys. Rev. B **73**, 155330 (2006).
[14] R. Ascazubi, I. Wilke, K. Dennison, H. Lu, and W. J. Schaff, Appl. Phys. Lett. **84**, 4810 (2004).
[15] I. Mahboob, T. D. Veal, C. F. McConville, H. Lu, and W. J. Schaff, Phys. Rev. Lett. **92**, 036804 (2004).
[16] G. Koblmüller, C. S. Gallinat, S. Bernardis, J. S. Speck, G. D. Chern, E. D. Readinger, H. Shen, and M. Wraback, Appl. Phys. Lett. **89**, 071902 (2006).
[17] E. O. Kane, J. Phys. Chem. Solids **1**, 249 (1957).
[18] D. L. Scharfetter and H. K. Gummel, IEEE Trans. Electron Devices **16**, 63 (1969).

Downloaded 25 Apr 2007 to 128.111.179.5. Redistribution subject to AIP license or copyright, see http://apl.aip.org/apl/copyright.jsp